Journal of Clinical Immunology (2022) 42:582–596
https://doi.org/10.1007/s10875-021-01176-3

ORIGINAL ARTICLE

Low Density Granulocytes and Dysregulated Neutrophils Driving Autoinflammatory Manifestations in NEMO Deficiency

Naz Surucu Yilmaz[1] · Sevgi Bilgic Eltan[2,3,4] · Basak Kayaoglu[1] · Busranur Geckin[1] · Raul Jimenez Heredia[5,6,7,8] · Asena Pinar Sefer[2,3,4] · Ayca Kiykim[9] · Ercan Nain[2,3,4] · Nurhan Kasap[2,3,4] · Omer Dogru[10] · Ayse Deniz Yucelten[11] · Leyla Cinel[12] · Gulsun Karasu[13] · Akif Yesilipek[13] · Betul Sozeri[14] · Goksu Gokberk Kaya[15] · Ismail Cem Yilmaz[1] · Ilayda Baydemir[1] · Yagmur Aydin[1] · Deniz Cansen Kahraman[16] · Matthias Haimel[5,7] · Kaan Boztug[5,6,7,8,17] · Elif Karakoc-Aydiner[2,3,4] · Ihsan Gursel[15] · Ahmet Ozen[2,3,4] · Safa Baris[2,3,4] · Mayda Gursel[1]

Received: 5 April 2021 / Accepted: 20 October 2021 / Published online: 14 January 2022

Abstract

NF-κB essential modulator (NEMO, IKK-γ) deficiency is a rare combined immunodeficiency caused by mutations in the *IKBKG* gene. Conventionally, patients are afflicted with life threatening recurrent microbial infections. Paradoxically, the spectrum of clinical manifestations includes severe inflammatory disorders. The mechanisms leading to autoinflammation in NEMO deficiency are currently unknown. Herein, we sought to investigate the underlying mechanisms of clinical autoinflammatory manifestations in a 12-years old male NEMO deficiency (EDA-ID, OMIM #300,291) patient by comparing the immune profile of the patient before and after hematopoietic stem cell transplantation (HSCT). Response to NF-kB activators were measured by cytokine ELISA. Neutrophil and low-density granulocyte (LDG) populations were analyzed by flow cytometry. Peripheral blood mononuclear cells (PBMC) transcriptome before and after HSCT and transcriptome of sorted normal-density neutrophils and LDGs were determined using the NanoString nCounter gene expression panels. ISG15 expression and protein ISGylation was based on Immunoblotting. Consistent with the immune deficiency, PBMCs of the patient were unresponsive to toll-like and T cell receptor-activators. Paradoxically, LDGs comprised 35% of patient PBMCs and elevated expression of genes such as *MMP9*, *LTF*, and *LCN2* in the granulocytic lineage, high levels of IP-10 in the patient's plasma, spontaneous ISG15 expression and protein ISGylation indicative of a spontaneous type I interferon (IFN) signature were observed, all of which normalized after HSCT. Collectively, our results suggest that type I IFN signature observed in the patient, dysregulated LDGs and spontaneously activated neutrophils, potentially contribute to tissue damage in NEMO deficiency.

Keywords NEMO deficiency · Autoinflammation · Low-density granulocytes · Neutrophil activation related genes · Interferon stimulated genes (ISGs)

Introduction

The NF-κB essential modulator (NEMO, IKKγ) is the regulatory subunit of the inhibitor of κB kinase (IKK) complex, responsible for phosphorylating the inhibitor of κB, thereby facilitating the release and translocation of the transcription factor NF-κB from the cytosol into the nucleus [1]. Once in the nucleus, NF-κB induces the expression of pro-inflammatory genes in order to prime immune cells and prevent emerging infections [2]. NF-κB is not only essential in pattern recognition receptor-mediated inflammatory responses but is also a key transcription factor in effector T cell activation and specific antibody generation in B-cells [3]. The broad range of cellular functions involving the activation of NF-κB such as survival, inflammation and apoptosis, illustrates the necessity for a functional NEMO protein [4].

X-linked NEMO deficiency is caused by hypomorphic mutations in the *IKBKG* gene [5], resulting in partial protein function and presents at infancy with ectodermal dysplasia

Naz Surucu Yilmaz, Sevgi Bilgic Eltan and Basak Kayaoglu contributed equally to this work. Mayda Gursel and Safa Baris contributed equally to this work.

✉ Safa Baris
safabaris@hotmail.com

✉ Mayda Gursel
mgursel@metu.edu.tr

Extended author information available on the last page of the article

(EDA) in males, commonly identified by sparse hair, hypohidrosis, and characteristic conical teeth [6], whereas females suffer from incontinentia pigmenti (IP) with abnormal skin involvement and skewed X-inactivation [7, 8]. These symptoms are accompanied by immunodeficiency (EDA-ID) [6], causing severe recurrent infections in early childhood, the most prominent of which are instigated by encapsulated pyogenic bacteria such as *Streptococcus pneumoniae* and *Haemophilus influenza.* Viral infections, *Pneumocystis*, and weakly mycobacterial infections resulting in multi-organ dissemination have also been described [6, 8, 9]. Previous studies reported autoinflammatory and autoimmune manifestations like inflammatory bowel disease, arthritis, Behcet's disease, panniculitis, and cytopenia in NEMO deficiency [10–13]. Furthermore, elevated levels of inflammatory markers without documented infection, mimicking autoinflammatory diseases, were also reported in this disease [14]. Increased TNF-α related apoptosis in epithelial cells of mice lacking NEMO has been proposed to govern gut bacterial translocation, leading to colitis [15]. Some reported mutations also pose partial TNF-α and toll-like receptor (TLR) cellular responses, contributing to the hyperinflammation [11, 16]. However, the mechanisms underpinning the exaggerated autoinflammatory symptoms in NEMO deficiency are not fully understood and need further investigation.

Low-density granulocytes (LDGs) were first characterized by Denny et al. in 2010 as a distinct subtype of neutrophils that are prematurely released from the bone marrow and promote pathogenesis in systemic lupus erythematosus (SLE) patients [17–19]. Notably, elevated IFN-α synthesized by LDGs was identified to exacerbate the pathophysiology in SLE patients [17, 20]. While type I IFNs are crucial cytokines in battling viral infections, they also have the capacity to exert detrimental effects when secreted uncontrollably. Type I interferonopathies like SLE, Aicardi-Goutieres syndrome or STING-associated vasculopathy with onset in infancy (SAVI), display the damaging potential of dysregulated type I IFN production and secretion [21]. In this context, we propose that the presence of LDGs, dysregulated neutrophil activation and a high type I IFN signature, likely account for autoinflammatory manifestations observed in NEMO deficiency.

Herein, we sought to investigate the underlying mechanisms of the autoinflammatory manifestations characterized by hyperemic nodular skin lesions, subcutaneous swelling, and pathologically reflected as perivascular and interstitial neutrophilic infiltrations with vacuolar degeneration, reminiscent of SLE skin involvement in NEMO deficiency. We show that the patient displayed high levels of dysregulated LDGs and spontaneously activated neutrophils due to an elevated type I interferon (IFN) signature, and propose that these abnormal cell populations carry the potential to inflict tissue damage in NEMO deficiency.

Methods

The Demographic and Clinical Data

The demographic and clinical features of the patient were retrieved from his medical records. These records included clinical history and laboratory test results.

Flow Cytometric Analysis

Peripheral lymphocyte subset analyses were performed by flow cytometry as described previously [22, 23]. For LDGs detection, peripheral blood mononuclear cells (PBMCs) were incubated with fluorochrome conjugated antibodies against CD14, CD15, CD16 and CD66b (all from BioLegend, USA) for 30 min at + 4 °C in the dark, with subsequent washing using FACS buffer (1% BSA, 0.2% NaN_3 in PBS) twice at 300 g for 10 min at + 4 °C. As such stained samples were then analyzed with a flow cytometer (NovoCyte 2060, Agilent Technologies). The details are provided in the Supplementary Material file.

Genetic Analysis

Targeted next-generation sequencing (NGS) was run on genomic DNA of the proband, as described earlier [24]. The details are provided in the Supplementary Material file.

RNA Isolation and NanoString Gene Expression Analysis

RNA from freshly isolated PBMCs ($2–4 \times 10^6$) were isolated using TRIzol® extraction. Quantity and quality of RNA samples were measured with NanoDrop™2000 (Thermo Scientific Fisher, USA). NanoString nCounter Inflammation and PanCancer Immune Profiling panels were utilized for gene expression [25]. Data analysis was carried out with the nSolver Analysis Software 4.0.

Results

A NEMO-Deficient Case with Autoinflammatory Skin Disorder

A 12-year-old born to non-consanguineous parents was referred to our Pediatric Immunology clinic at 18 months because of possible immunodeficiency. The patient's medical history was remarkable for sepsis at newborn period and hospitalization due to bronchopneumonia at 4 months of age. At admission, physical examination revealed signs of moniliasis, EDA

findings were characterized by hyperpigmented skin, weak and sparse hair, eyebrows and eyelashes, conical-shaped teeth and micrognathia (Fig. 1a). His mother had incontinentia pigmenti (Fig. 1b) without any other complaints. In his family history there was a cousin with anhidrosis and recurrent otitis media without genetic background.

His initial laboratory examination revealed high white blood cell count and anemia accompanied by coombs positivity. We detected non-protective protein vaccine responses (anti-Hbs, anti-varicella IgG, anti-rubella IgG, anti-measles IgG) and polysaccharide isohemagglutinin levels (Table 1). He demonstrated hypergammaglobulinemia with low $CD3^+$ and $CD4^+$T cells and decreased T cell proliferation in response to PHA compared to healthy controls. The autoantibodies including anti-nuclear antibody and anti-dsDNA were negative. During the follow-up, lung computed tomography showed infiltration on the posterior segment of the upper lobe of right lung, concomitant with 2 × 3-cm-sized bilateral axillary lymphadenopathies (LAPs). Cervical LAP biopsy exhibited necrotizing granulomatous lymphadenitis with positivity for *Mycobacterium tuberculosis*. He was commenced on anti-tuberculosis treatment for 6 months. Later, he developed left femoral diaphysis osteomyelitis and fracture complicated with abscess formation. *Streptococcus pneumonia* was isolated from the abscess culture. Next-generation sequencing identified a previously known hemizygous missense mutation in the exon 5 of *IKBKG* gene (c.613C > T; NM_001099857.5), leading to premature stop codon (p.Gln205*; NP_001093327) [26].

At the age of 3 years, and in view of unrelenting disease course, the patient underwent transplantation using 5/6 mismatch unrelated cord blood donor. The patient received a myeloablative conditioning regimen with busulfan and fludarabine. Cyclosporine and anti-thymocyte globulin were used for graft-versus-host disease (GvHD) prophylaxis. After transplantation, blood cytomegalovirus (CMV) remained negative and chimerism was 36% and 43% at 1 and 3 months, respectively. At 2 months of post-transplantation, he developed acute GVHD and colitis, treated with systemic corticosteroid (CS). However, thereafter, his chimerism progressively decreased and became non-chimeric (both lymphoid and myeloid) for 3 years. During this period, he was hospitalized twice due to systemic CMV infection complicated with lung involvement, required prolonged ganciclovir therapy. He also developed severe intractable mucositis and aphthous stomatitis, complicated with fever.

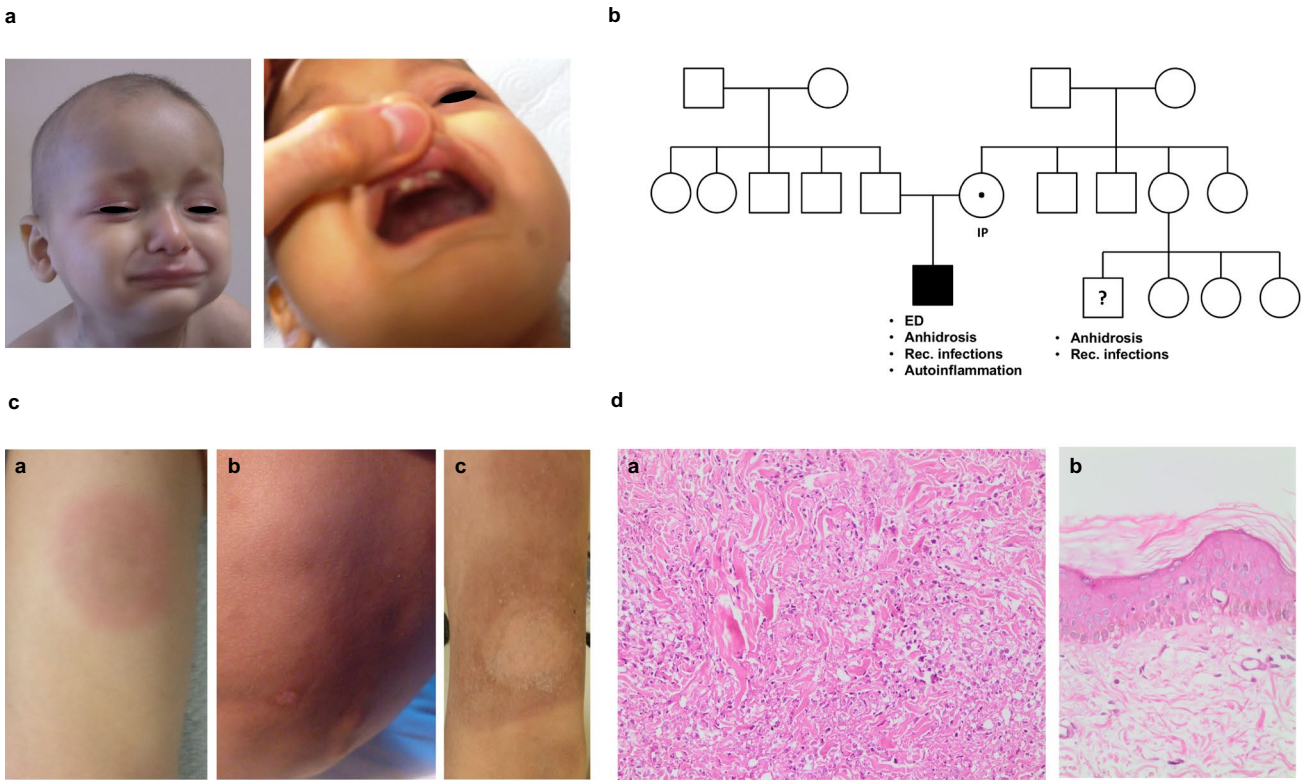

Fig. 1 The clinical features and family pedigree of the patient with NEMO deficiency. **a)** The typical findings of ectodermal dysplasia including sparse hair, eyebrows and eyelashes, conical-shaped teeth and micrognathia. **b)** Extended pedigree information of the family (IP, incontinentia pigmenti; ED, ectodermal dysplasia). **c)** Skin lesions during the acute phase (hyperemic nodular lesions, a and b) and after healing (hyperpigmentation, c) of the autoinflammatory disorder. **d)** Skin biopsy with hematoxylin and eosin staining shows dermal extensive neutrophilic infiltration (a, 20×) and basal membrane vacuolar degeneration (b, 40×)

Table 1 The clinical and laboratory findings of NEMO-deficient patient

Parameters	1st admission (4 months)	Reference values (0–2 years)	After 1st HSCT (3 years)	Reference values (3–4 years)	After 1st HSCT (5 years)	Reference values (5–6 years)	Before 2nd HSCT (8 years)	Reference values (7–8 years)	After 2nd HSCT (12 years)	Reference values (9–13 years)
Infections	*Mycobacterium tuberculosis*	Herpes simplex virus, oral candidiasis	-	-	Oral candidiasis, *Klebsiella* pneumonia, cytomegalovirus	-	-	-	-	-
Autoinflammation	-	-	-	-	Aphthous stomatitis	-	Recurrent fever with skin involvement (sweet syndrome-like lesions)	-	-	-
Leucocyte (µ/L)	**18,650**	2500–17,800	3400	5000–15,500	6900	5000–15,500	5900	4500–13,500	**3900**	4500–13,500
Absolute lymphocyte (µ/L)	7900	3260–8840	**800**	2430–6060	2400	2130–4500	**900**	1750–3460	1720	1710–3060
Absolute neutrophil (µ/L)	**8900**	1000–8500	2100	1500–8000	3700	1500–8000	4800	1500–8500	**1400**	1500–8500
Hb (g/dl)	8.7	7.2–12.7	**6.9**	11.5–13.5	13.7	1.5–13.5	12	11.5–15.5	11.7	11.5–15.5
Platelets (µ/L)	510,000	140,000–635,000	**473,000**	150,000–350,000	253,000	150,000–350,000	**485,000**	150,000–350,000	218,000	150,000–350,000
Protein vaccine responses	**Negative**	Positive	**Negative**	Positive	**Negative**	Positive	ND	-	Positive	Positive
Isohemagglutinin (anti-A and anti-B)	**1/2 (for both)**	N > 1/8	ND	-	ND	-	ND	-	ND	-
IgG; mg/dl	**3130**	633–1466	ND	-	867	745–1804	1052	764–2134	921	842–1943
IgA; mg/dl	**725**	11–14	ND	-	**364**	57–282	**474**	78–383	324	62–398
IgM; mg/dl	**112**	22–87	ND	-	**41**	78–261	**30**	69–387	**49**	54–392
IgE; IU/ml	**424**	0–50	ND	-	10.2	0–50	40.8	0–50	23	0–50
$CD3^+$T, cell/µL	2686	1850–5960	**576**	1500–3870	1800	1420–3120	**612**	1360–2740	**848**	1070–2270
$CD3^+CD4^+$T, cell/µL	1580	1140–3800	**176**	880–2360	1080	540–1840	**459**	660–1610	**523**	640–1290
$CD3^+CD8^+$T, cell/µL	1106	540–1970	**384**	410–1280	696	470–1200	**153**	440–1050	**304**	380–880
$CD19^+$B, cell/µL	**200**	640–1960	**0**	310–1130	480	260–970	243	200–680	474	170–630
$CD16^+56^+$NK, cell/µL	**79**	150–1330	**128**	150–810	**58**	180–510	**37.8**	150–510	170	170–530

Table 1 (continued)

Parameters	1st admission (4 months)	Reference values (0–2 years)	After 1st HSCT (3 years)	Reference values (3–4 years)	After 1st HSCT (5 years)	Reference values (5–6 years)	Before 2nd HSCT (8 years)	Reference values (7–8 years)	After 2nd HSCT (12 years)	Reference values (9–13 years)
Naive B cells, %	ND	-	ND	-	**89**	65–86	83	51–85	86	64–84
NCS B cells, %	ND	-	ND	-	**2.6**	5–16	7.4	5–17	5.4	4–14
CS B cell, %	ND	-	ND	-	2	2–16	7.1	5–22	**2.9**	6–16
$CD4^+CD45RA^+CCR7^+$ T, %	ND	-	ND	-	**83**	35–69	**78**	32–68	34	25–63
$CD4^+CD45RA^-CCR7^+$ T, %	ND	-	ND	-	12.8	9–25	17.6	9–24	**10**	11–25
$CD4^+CD45RA^-CCR7^-$ T, %	ND	-	ND	-	**1.8**	10–30	**3.7**	9–32	**47.8**	12–30
$CD4^+CD45RA^+CCR7^-$ T, %	ND	-	ND	-	**2**	4–22	**0.09**	4–15	6.3	4–24
$CD8^+CD45RA^+CCR7^+$ T, %	ND	-	ND	-	**90**	23–68	**88**	30–61	31	22–58
$CD8^+CD45RA^-CCR7^+$ T, %	ND	-	ND	-	**1.8**	4–11	**1.13**	2–12	2,9	2–15
$CD8^+CD45RA^-CCR7^-$ T, %	ND	-	ND	-	**2.4**	14–59	**6.1**	20–45	44	24–58
$CD8^+CD45RA^+CCR7^-$ T, %	ND	-	ND	-	**5.2**	6–30	**3.8**	7–26	21	7–26
T cell proliferation (anti-CD3 stimulated)	**10**	> 50%	78	> 50%	**18**	> 50%	ND	-	64	> 50%
CRP (mg/L)	ND	-	**15**	0–5	3.2	0–5	**92**	0–5	**16.7**	0–5
ESR (mm/h)	ND	-	ND	-	**37**	0–10	**107**	0–10	ND	-
Chimerism (%)	ND	-	46	0–100	35	0–100	0	0–100	100	0–100

CSB class-switched memory B cells, *CRP* C-reactive protein, *ESR* erythrocyte sedimentation rate, *NCS B* non-class-switched memory B cells, *ND* not done

The abnormal values are indicated in bold

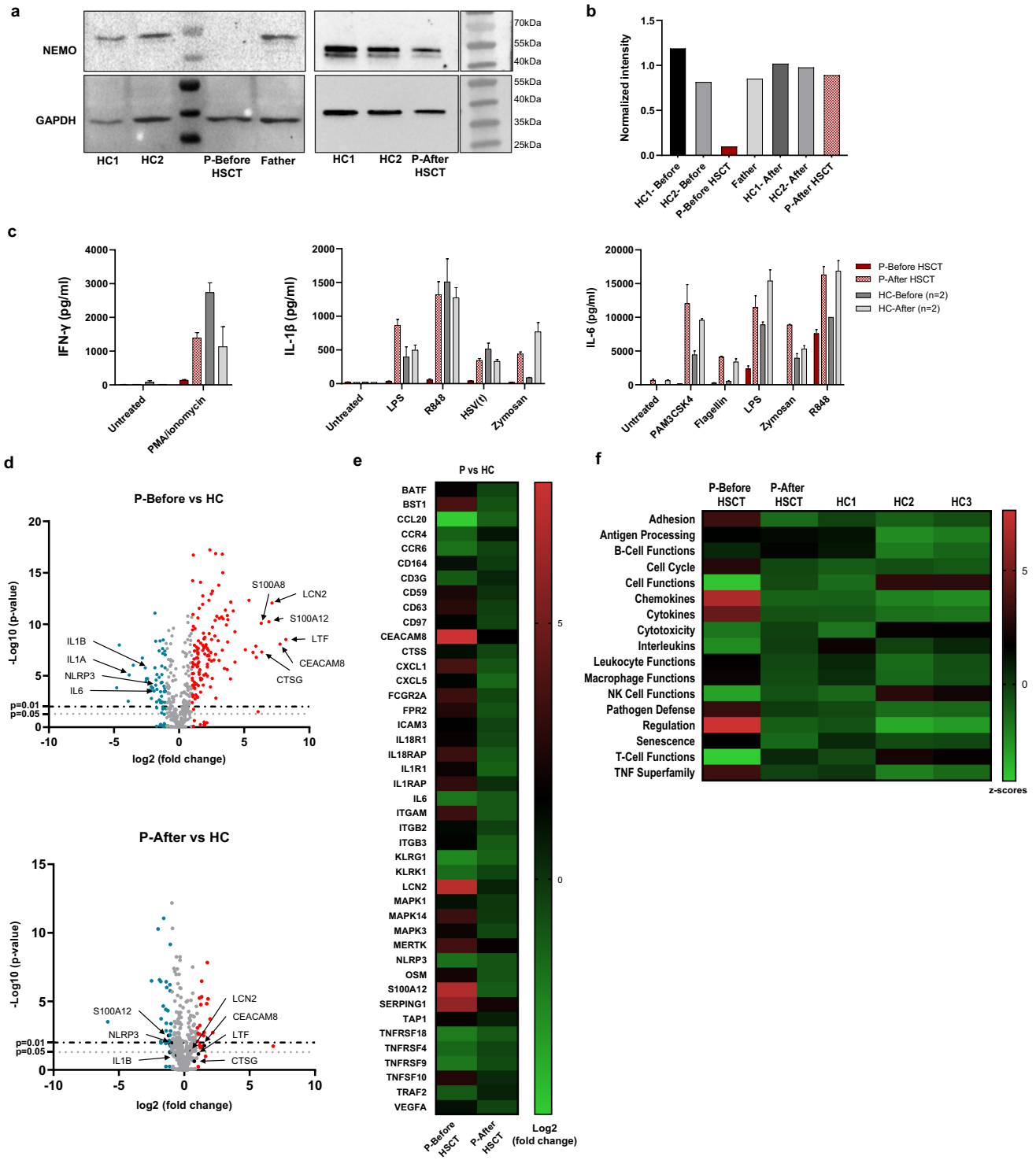

At 8 years of age, he started to experience recurrent fever accompanied by hyperemic, painful nodular skin lesions with subcutaneous swelling (Fig. 1c). Skin biopsy showed epidermal apoptotic keratinocytes, focal vacuolar degeneration and perivascular and interstitial neutrophilic infiltration reminiscent of sweet syndrome or SLE-like disorder (Fig. 1d). He did not experience gastrointestinal involvement. His symptoms were partially controlled by oral CS and colchicum and the lesions healed with hyperpigmentation (Fig. 1c). During this period, peripheral blood samples from the patient were subjected to detailed functional analyses as described in the following sections. Autoinflammatory disorder was considered due to recurrent fever without documented infectious agent, skin lesions and high acute

◂**Fig. 2** The NEMO-deficient patient exhibits impaired cellular functions and granulocyte specific gene expression in PBMCs. **a–b)** Immunoblot analysis (a) and quantification (b) of NEMO protein in PBMC lysates including four unrelated healthy controls (HC), the father of the patient (Father), and the patient (P-Before HSCT or P-After HSCT). The anti-IKKγ antibody employed in these experiments was specific to the C-terminal of the protein. Normalizations were conducted first by dividing the adjusted intensity of NEMO bands by the intensities of GAPDH bands for each individual. Secondly, the housekeeping normalized values were divided by the average of healthy controls and are shown as bar graphs. Molecular weights are indicated at the right side of the ladder images. **c)** Culture supernatant ELISA results of IFN-γ, IL-1β, and IL-6 from 24-h stimulated PBMCs of the patient before (P-Before HSCT) and after HSCT (P-After HSCT) and unrelated healthy controls (HC, $n=2$). HC-Before ($n=2$), and HC-After ($n=2$) represent healthy controls that were studied together with the patient's samples before or after transplantation, respectively. **d)** Volcano plots of differentially expressed genes between the patient and healthy controls ($n=3$) PBMCs' before (top) and after (bottom) HSCT. Upregulated (fold change ≥ 2) and downregulated (fold change ≤ 2) genes are shown in red and blue, respectively. Black arrows show corresponding dots of indicated genes. In the bottom graph the normalized genes are indicated with black dots. Dashed lines represent $P=0.01$ and dotted lines show $P=0.05$. **e)** Heat map with fold change showing differentially expressed genes between the patient and healthy controls ($n=3$) before (P-Before HSCT) and after (P-After HSCT) transplantation. **f)** Heat map and clustering analysis of z-scores showing differential gene expression of PBMCs for different pathway sets in NEMO-deficient (P-Before HSCT), NEMO reconstituted (P-After HSCT) patient and healthy controls (HC)

phase reactants (Table 1). He was unresponsive to anti-IL-1 targeted therapy. At 9 years of age, owing to the recurrent infections and uncontrolled autoinflammatory manifestations, we decided to re-transplant him from full-matched unrelated donor. Hematological recovery was achieved and there were no signs of acute or chronic GvHD. He is now at 3 years after transplantation with continued 100% donor chimerism without sign of autoinflammation. As discussed later, peripheral blood cells were again subjected to functional analyses at 9 months post-transplantation for comparison with pre-transplant cellular responses.

The Nonsense Mutation Observed in the Patient Corresponding for the Disease Phenotype

Western blot analysis of PBMCs showed loss of full-length NEMO protein compared to healthy controls and father of the patient, which normalized after transplantation (Fig. 2a, b), confirming the deleterious effect of the c.613C > T mutation. We evaluated the functional capacity of NF-κB signaling initiated by TLR and T cell receptor (TCR) activation. Stimulation of NEMO-deficient and healthy PBMC samples with TLR2 (PAM3CSK4, zymosan), TLR4 (LPS), TLR5 (flagellin), and TLR7/8 (R848) agonists confirmed that the patient had lower IL-6 and IL-1β secretion compared to healthy controls, demonstrating the insufficiency of NF-κB dependent innate immune activation (Fig. 2c). Importantly, we observed that IL-6 levels in the patient were similar to those observed in healthy controls upon R848 (resiquimod) stimulation, demonstrating partial NF-κB activation ability. This result suggests that the unresponsiveness to other stimuli in the patient does not stem from low viability of PBMCs (Fig. 2c). Furthermore, NEMO-deficient PBMCs failed to secrete IFN-γ in response to PMA/ionomycin treatment mimicking TCR signaling through protein kinase C activation, thereby showing incomplete NF-κB signal transduction for T cell activation (Fig. 2c). As expected, cytokine responses were restored to healthy levels after HSCT (Fig. 2c). Consequently, our results show that innate immune functions and T cell-mediated immunity in the NEMO-deficient patient were compromised due to the NEMO deficiency, but improved successfully after transplantation.

Baseline Targeted Transcriptional Gene Expression Analysis of PBMCs from NEMO-Deficient Patient Reveals Neutrophil Activation Signature, Normalized After Transplantation

To delineate possible mechanisms that might account for the systemic inflammatory manifestations observed in the patient during the pre-transplantation period, we assessed alterations in PBMC gene expression patterns before and after transplantation, using the NanoString Inflammation and PanCancer Immune Profiling panels. Consistent with the patient's clinical course, NF-κB activation inducible genes like *IL1B*, *IL1A*, *IL6*, *NLRP3* were downregulated in resting PBMCs of the patient (Fig. 2d, e; Fig. S1a, b) prior to transplantation. Furthermore, inflammation associated genes, especially of the chemokine family such as *CXCL1* and *CXCL5* were upregulated (Fig. 2e; Fig. S1a, b). Interestingly, genes related to neutrophil-derived granule proteins and neutrophil function including, *lactoferrin (LTF)*, *lipocalin-2* (*LCN2*), *S100 calcium-binding protein A12* (*S100A12), matrix metallopeptidase 9 (MMP9)* and *alpha defensin 1* (*DEFA1), carcinoembryonic antigen-related cell adhesion molecule 8 (CEACAM8), serpin family G member 1 (SERPING1), cathepsin G (CTSG)* were differentially upregulated in patient PBMCs prior to transplantation (Fig. 2d; Fig. S1a, b). Pathway enrichment analysis revealed significant upregulation in gene groups associated with adhesion, chemokines, leukocyte and macrophage functions (Fig. 2f; Fig. S1c–f). The dysregulated gene expressions were normalized after transplantation (Fig. 2d, e). Overall, the gene expression pattern of the patient before transplantation indicates the activation of inflammatory pathways and neutrophil-related functions in spite of the persistent immunodeficiency and the absence of active infection.

LDGs Detected in PBMCs of the NEMO-Deficient Patient Exhibit Neutrophil Activation Signature

Since we observed prominent neutrophilic infiltration in the inflamed skin area and elevated neutrophil activation-associated genes, including *MMP9*, *LTF*, and *LCN2* in the patient during the pre-transplantation period, where systemic inflammatory manifestations were apparent, we next sought to assess the involvement of a subset of proinflammatory neutrophils known as LDGs as a mediator of this inflammation. LDGs were characterized in the isolated PBMC fraction of the patient by flow cytometry based on the expression of neutrophil but not monocyte-specific cell surface markers. Since LDGs are of granulocytic origin, they do not express the monocyte specific surface protein CD14 but display granulocyte specific CD15 and CD16 [27]. Furthermore, CD66b (CEACAM8) is a granulocyte activation marker that is dimly expressed on resting neutrophils and thereby enables the separation of LDGs from conventional neutrophil contamination in PBMCs [28]. As expected, flow cytometric analysis revealed that the LDG percentage in PBMCs of healthy controls remained between 0–2%, whereas the patient had 34–35% $CD14^{dim}CD15^{hi}$, $CD15^{hi}CD66b^{hi}$, and $CD14^{dim}CD66b^{hi}$ cell populations, demonstrating the presence of active circulating LDGs (Fig. 3a, b). Furthermore, the LDG population was still present after 5 months of our initial detection, suggesting that LDG generation in this patient was not an acute but a chronic event (Fig. S1g). Parallel to the resolution of inflammation, LDG numbers in the patient returned to baseline healthy control levels at 9 months post-transplantation (Fig. 3a, b).

Previous studies regarding gene expression patterns of LDGs from SLE patients, demonstrate significant differences between LDGs and autologous or healthy neutrophils and show that LDGs display enhanced expression of IFN-stimulated genes (ISGs) [17, 29–31]. To gain further insight into the nature of LDGs in the NEMO-deficient patient, we sorted and isolated LDGs and compared their gene expression levels to healthy neutrophils. Targeted transcriptomic analysis revealed differential regulation of a total of 120 genes. Of these, 78 and 42 genes were up- and down-regulated, respectively (Fig. S2a, b). Strikingly, expression levels of *LTF* and *LCN2* genes encoding for lactoferrin and neutrophil gelatinase-associated lipocalin were upregulated 870 and 330-fold, respectively (Fig. 3c, d). These proteins are major antimicrobial agents of the innate defense system that are considered as markers of neutrophilic inflammation [32]. Furthermore, the genes associated with neutrophil recruitment, such as those encoding for the adhesion molecules CEACAM8 (CD66b), CEACAM6 (CD66c) or S100 protein family members like S100A8 and S100A12 were upregulated 170, 80, 5 and 30-fold, respectively [33–36] (Fig. 3c, d). S100A8 and S100A12 are overexpressed and secreted from neutrophils during inflammation and were found to be associated with the pathogenesis of the auto-inflammatory condition Familial Mediterranean Fever [33, 36]. Our data demonstrates that LDGs, unlike resting healthy neutrophils, overexpress genes associated with inflammation, adhesion, and antimicrobial defense, illustrating their potential capability in promoting pathogenesis in NEMO deficiency (Fig. S3a, b). Considering the given data and that the patient's clinical autoinflammatory manifestations disappeared gradually after HSCT in parallel with the decline in the LDG population (Fig. 3a, b, Fig. S2c), our results strengthen the notion that LDGs were involved in the auto-inflammatory pathophysiology in NEMO deficiency.

Dysregulated Neutrophil Activation in NEMO Deficiency Was Corrected with HSCT

Since the presence of LDGs is indicative of abnormal neutrophil development, we further examined the activation status of NEMO-deficient normal density neutrophils by comparing their reactive oxygen species (ROS) content to healthy neutrophils and assessed their potential involvement in the pathophysiology of NEMO deficiency. Neutrophil response mechanisms essentially include the formation of ROS through the enzymatic activity of NADPH-oxidase to facilitate the killing of invader pathogens [37, 38]. Flow cytometric analysis showed that 40% of unstimulated NEMO-deficient neutrophils were positive for intracellular ROS in comparison to untreated healthy neutrophils, illustrating that NEMO-deficient neutrophils acquired a spontaneously primed state (Fig. 4a, b, Fig. S3c, d). PMA treated neutrophils from both the patient and healthy controls were 99% positive for DHR123 (Fig. S3c, d). Following HSCT, ROS levels in unstimulated patient neutrophils returned to normal levels (Fig. 4a, b). Consistent with our flow cytometric analysis, targeted transcriptomics data revealed that genes associated with adhesion and pathogen defense were differentially upregulated in NEMO-deficient normal density neutrophils (Fig. 4c, Fig. S3a, b). Specifically, we observed around 16 and 13-fold upregulation in the *CYBB* and *CTSG* genes, encoding for p91-phox and cathepsin G, respectively (Fig. 4d). While the former is a subunit of the transmembrane enzyme complex NADPH-oxidase, the latter is a serine protease found in azurophilic granules of neutrophils [39]. Similarly, expression of the adhesion molecules CEACAM8 and CEACAM6 was elevated 22 and 13-fold, respectively (Fig. 4d). Consistent with the disappearance of the LDG population, neutrophil gene expression signatures returned to healthy neutrophil levels post-HSCT (Fig. 4d). Our data underline the primed status of NEMO-deficient neutrophils and assert their capacity to adhere and infiltrate target tissues, and contribute to the pathophysiology of auto-inflammation in NEMO deficiency.

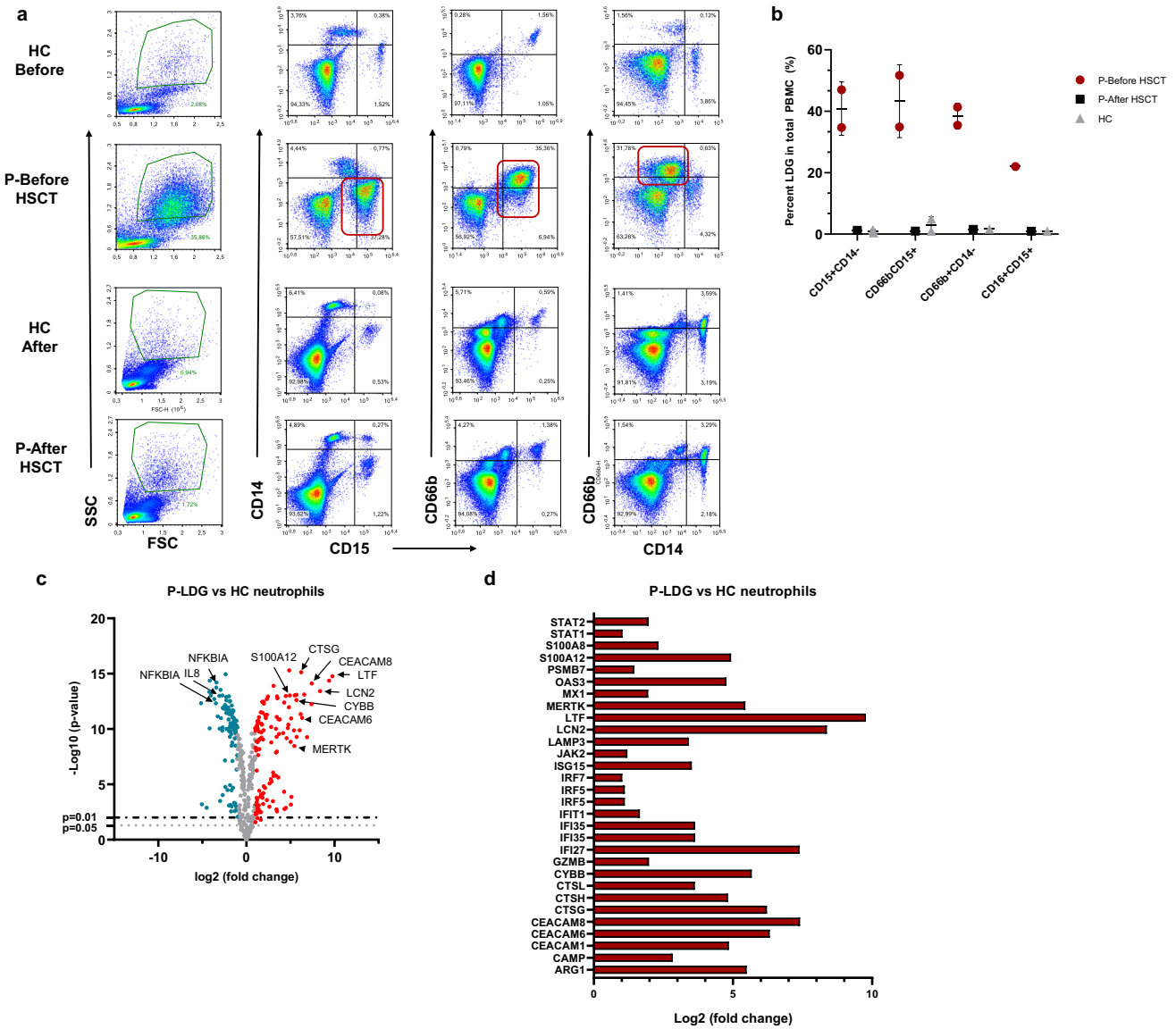

Fig. 3 LDGs in the PBMC of the NEMO-deficient patient show differential gene expression compared to healthy neutrophils. **a)** Flow cytometric analysis of PBMCs from the patient and healthy controls before and after HSCT. Columns from left to right illustrate, FSC-SSC, CD15 and CD14, CD15 and CD66b, CD14 and CD66b density plots. Red rectangles depict the LDG population observed in the patient PBMCs. Rows from top to bottom show different staining combinations for each individual. HC-Before represents the healthy control that was used in the experiments done before HSCT. HC-After shows the healthy control that was used in the experiments done after HSCT. **b)** Graph showing LDG marker percentages from (a) and S1g. **c)** Volcano plot of differentially expressed genes between the patient's LDGs and healthy neutrophils. Upregulated (fold change ≥ 2) and downregulated (fold change ≤ 2) genes are shown in red and blue, respectively. Dashed line represents P = 0.01 and dotted line shows $P = 0.05$. **d)** Bar graph depicting selected differentially expressed genes (DEG) in LDGs from the NEMO-deficient patient (P-LDG) compared to healthy neutrophils (HC)

Spontaneous Type I IFN Signature in the NEMO-Deficient Patient Subsides After HSCT

Type I IFNs have previously been shown to exert an activatory effect on neutrophils [40]. In this context, we explored the involvement of type I IFNs in priming of neutrophils in the patient. We compared plasma circulating IP10 (CXCL10, IFN-γ inducible protein 10) levels in the patient and healthy controls, and observed at least five-fold higher concentrations in the patient (Fig. 4e; Fig. S3e, f). Approximately five-fold enhanced *CXCL10* expression in the patient was also evident in the differential gene expression analysis conducted by comparing NEMO-deficient and healthy PBMCs (Fig. 4f). We also detected higher levels of IFN-α in the plasma of the patient when compared to healthy plasma samples (Fig. S3e).

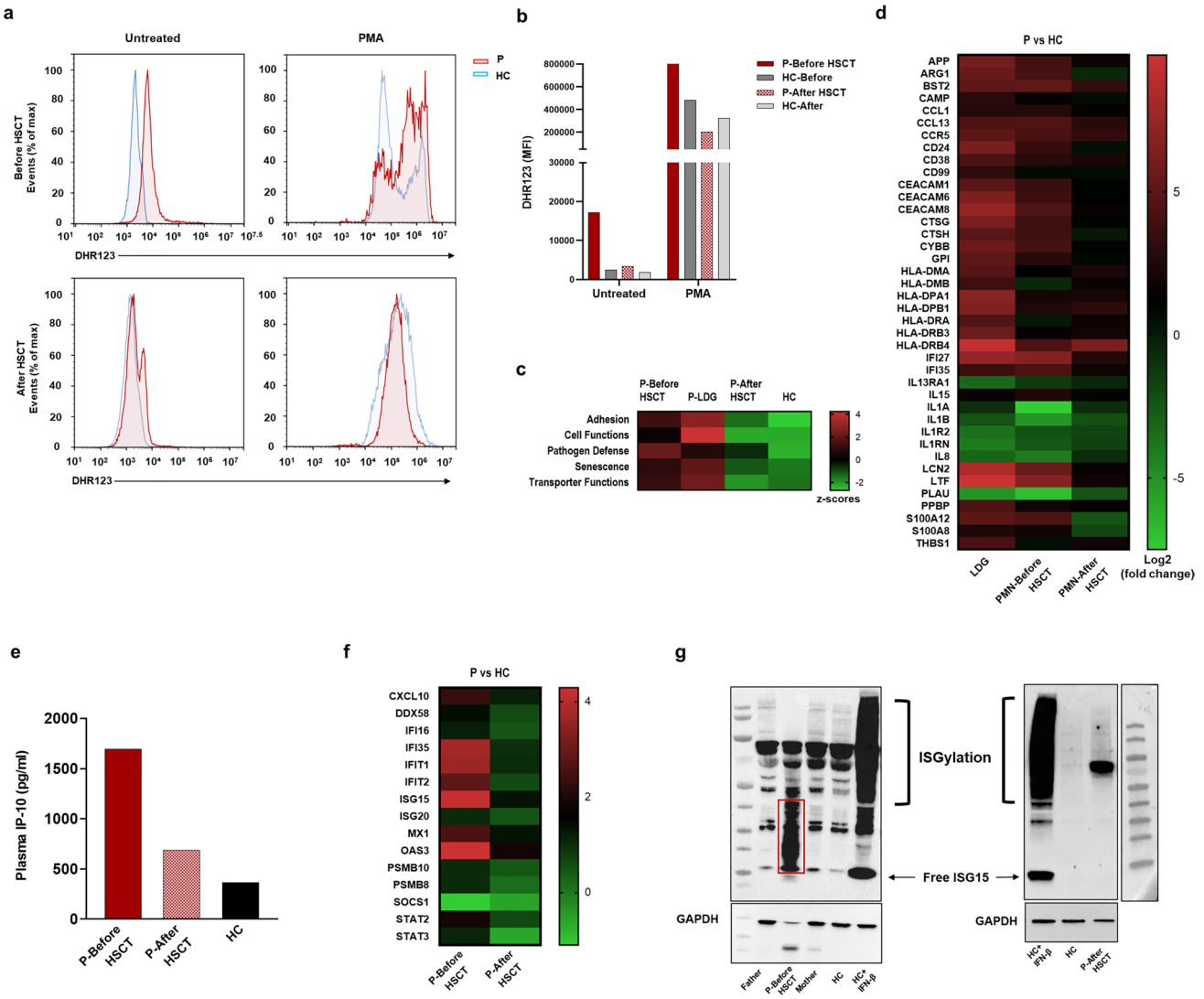

Fig. 4 Spontaneous neutrophil activation and elevated type I IFN signatures in NEMO deficiency. **a)** Flow cytometric analysis of DHR123 staining. Histograms depicting DHR123 staining of untreated or PMA (15-min) stimulated neutrophils before and after transplantation. The patient (P) is shown in red and healthy control (HC) is shown in blue. Upper two histograms display the experiment conducted before HSCT while the bottom two show the experiment after HSCT. **b)** Bar graphs of the mean fluorescence intensities of DHR123 positive cells shown in (a). **c)** Heat map and clustering analysis of z-scores displaying differential gene expression of different pathway sets expressed in LDGs (P-LDG), NEMO-deficient (P-Before HSCT), NEMO reconstituted (P-After HSCT) and healthy (HC) neutrophils. **d)** Heat map showing $\log_2$(fold change) of differentially expressed genes between LDGs (LDG) and autologous neutrophils of the patient before (PMN-Before HSCT) and after (PMN-After HSCT) transplantation on the baseline of healthy neutrophils (HC). **e)** Bar graph of ELISA results for IP10 levels in the plasma from the patient before (P-Before HSCT) and after transplantation (P-After HSCT), and healthy control (HC). **f)** Heat map with $\log_2$(fold change) showing type I IFN related differentially expressed genes between the patient and healthy controls ($n=3$) before (P-Before HSCT) and after (P-After HSCT) HSCT. **g)** Anti-ISG15 and anti-GAPDH immunoblots from the patient (P-Before HSCT, P-After HSCT), the patient's father (Father), the patient's mother (Mother) and healthy control's (HC) PBMC lysates before (left image) and after (right image) transplantation. Sample identifications are indicated at the bottom. Red rectangle indicates the ISGylated proteins observed in the patient's PBMCs. Black brackets between two images indicate ISGylated proteins in recombinant IFN-β-stimulated positive controls (HC + IFN-β)

Next, we compared interferon stimulated gene 15 (ISG15) expression and protein ISGylation as an indicator of type I IFN signaling in NEMO-deficient and healthy PBMCs. ISG15 is a ubiquitin-like protein that covalently binds other cellular proteins in a process called ISGylation in response to type I IFN signaling [41]. In its free form, ISG15 can exhibit antiviral activity and can act as a cytokine when released from cells [42, 43]. We observed spontaneous ISGylation of intracellular proteins and the presence of free ISG15 in untreated NEMO-deficient PBMC lysates (Fig. 4g). Elevated

IP10 levels and ISGylated proteins provide evidence that the patient displayed an enhanced type I IFN signature [44]. In addition to *CXCL10*, targeted transcriptome analysis of NEMO-deficient PBMCs showed upregulation of other interferon response genes, including *ISG15* (~17 fold), *MX1* (~6 fold), and *OAS3* (~19 fold), which returned to baseline levels after transplantation (Fig. 4f). Furthermore, after HSCT, circulating IP10 and free ISG15/ISGylated protein levels were indistinguishable compared to healthy controls. Our data indicates that NEMO deficiency can be linked to an elevated type I IFN signature, which in turn could be the source of expansion in LDGs and neutrophil activation.

Surprisingly, while preparing lysates from patient PBMCs, despite the addition of protease inhibitors, we observed protein degradation (Fig. 4g). We reasoned that given the intense LDG population present in the PBMC fraction and the 99-fold enhanced expression of MMP9 according to our inflammation panel analysis prior to HSCT (Fig. S1b), proteins in the prepared lysates might be degraded, affecting the outcome of immunoblotting experiments. In order to circumvent MMP activity and validate that the absence of NEMO prior to transplantation is not the result of protein degradation, we depleted LDGs and monocytes from the patient and healthy PBMCs and repeated immunoblotting against GAPDH, ISG15 and NEMO. ISG15 and ISGylated protein levels in NEMO-deficient PBMCs were confirmed to be elevated again (Fig. S3g). Similar to our initial result, we also verified the lack of NEMO protein in LDG/monocyte depleted pre-transplantation PBMCs (Fig. S3h). Of note, the immunoblots of undepleted and depleted PBMC lysates showing ISGylation in the patient were conducted 5 months apart, respectively, thereby confirming again the presence of a chronic inflammatory status.

Discussion

There has been extensive research on the characterization of various hypomorphic mutations in the *IKBKG* gene [45]. To date, the mechanistic events leading to autoinflammation in NEMO deficiency have not yet been fully examined. Herein, we explored for the first time the underlying mechanisms for autoinflammatory symptoms observed in a NEMO-deficient patient. Unleashing of ample amount of LDGs and spontaneously activated neutrophils, accompanied by elevated type I IFN signatures uncover a new model for the autoinflammation observed in NEMO deficiency.

IKK-γ/NEMO is a 419 amino acid protein that contains two coiled-coil (CC1 and CC2), leucine zipper (LZ), and zinc finger (ZF) motifs, enabling it to carry out pleiotropic functions dependent or independent of NF-κB signaling [46, 47]. The nonsense mutation in the patient had arisen at p.Gln205* excluding the CC2, LZ, and ZF motifs of IKK-γ, thereby leaving the CC1 domain responsible for its interaction with IKKα and IKKβ intact [48, 49]. Further variation analysis shows a homozygous variant for *DNAH5* and benign heterozygous variants for *RAB27A* and *TREX1* (Supplementary Table 1), which were not linked to clinical findings. Earlier studies suggest that the role of the C-terminal is associated with NEMO recruitment to upstream signaling molecules [50] and uses its CC2 and LZ domain for linear K63 polyubiquitin sensing in response to TNF-R1 activation [51]. As the complete absence of NEMO is embryonically lethal in males and our patient was unable to produce full-length NEMO before undergoing HSCT, he most likely was expressing a partially functional truncated NEMO protein capable of binding to IKKα and IKKβ but unable to interact with receptor-interacting protein (RIP) downstream of TNF-R1. Klemann et al. show an abundance of the NEMO isoform of 40 kDa lacking exon 5 due to alternative splicing, while the 48 kDa isoform is absent in a patient carrying the same mutation [26]. We tried to identify the 48 kDa NEMO protein or any of its isoforms that might have been utilized by the patient using alternative antibodies. Our initially employed C-terminal antibody did not reveal any protein bands in the patient, while showing clear 48 kDa bands and faint 40 kDa bands in healthy individuals (Fig. 2a, b). We also tried immunoblotting by using an alternative N-terminal specific antibody. While healthy individuals expressed two isoforms of NEMO, the patient's sample failed to show the 48 kDa protein or any isoforms (Fig**.** S3i). As the complete absence of NEMO is embryonically lethal and we could not identify a short-truncated protein or isoforms, we strongly think that due to the chronic inflammatory state of the patient it is likely that any residual NEMO that the patient had been utilizing is prone to rapid proteasomal degradation, thereby evading detection by immunoblotting. Due to restricted availability of patient samples the limitation of this study remained the determination of whether the patient utilized a shorter truncated NEMO protein without the CC2, LZ, ZF domains and/or the exon 5 lacking 40 kDa isoform resulting from alternative splicing leading to NEMO-NDAS [52].

Gene expression analysis performed with PBMC from the patient and healthy controls displayed differentially up/downregulation in immune sensing and signaling associated genes in the patient before HSCT. Patient cells showed less expression of NF-κB targeted pro-inflammatory genes such as *IL6, IL1A, IL1B, NLRP3,* consistent with impaired innate immune signaling (Fig. 2d, e; Fig. S1a, b). *CCL20*, a chemoattractant for activated T lymphocytes [53, 54] was downregulated in resting PBMC of the patient compared to healthy controls (Fig. 2e). Furthermore, transcripts from members of the TNF receptor superfamily such as TNFRSF4 and TNFRSF9, known to be upregulated upon T cell antigen

recognition [55], were also found to be lower in the patient's PBMC (Fig. 2e). In addition to the decrease in TRAF2 expression responsible for recruitment of the IKK complex to RIP-1 [56], the data suggest that the T cell signaling pathway in the patient was downmodulated before transplantation. In contrast, significant upregulation was observed in genes observed in the granulocytic lineage such as *LTF* and *LCN2* (Fig. 2d). Both are antimicrobial molecules stored in granules of neutrophils and released upon initiation of inflammation [57, 58]. Furthermore, a 22-fold increase of *CEACAM8* (CD66b) expression (Fig. 2d), an adhesion and activation marker that is upregulated on the surface of neutrophils following their activation [28] indicates the involvement of LDGs in the pathophysiology of the NEMO-deficient patient. The increased levels of *CTSG* (Fig. 2d), encoding for cathepsin G found in azurophilic neutrophils [59] also validates the presence of inflammation [60] and the contribution of LDGs to the autoinflammatory state of the patient. Moreover, elevated expression of interferon response genes such as *IFIT1, IFIT2, ISG15, OAS3,* and *MX1* (Fig. 4f) is consistent with a functional type I IFN signature in the patient evident by high IP-10 in the patient serum and ISGylation of intracellular proteins (Fig. 4e, g). Collectively, our gene expression data reveals the immune deficiency in innate immune signaling as well as T cell responses in the patient; it also is consistent with the neutrophil involved autoinflammatory manifestations.

Interestingly, although the patient was unable to secrete pro-inflammatory cytokines upon TLR activation, he could produce acute-phase proteins and experience recurrent fever. Moreover, while gene expression of *IL6* and *IL1B* was low in the patient, he had high amounts of TNF-α transcripts. This suggests that the truncated protein possibly mediated restricted tasks, but was still insufficient to carry out necessary functions of a fully competent innate and adaptive immune system.

Previously, it was reported that a major part of white blood cells in SLE patients consisted of immature neutrophils and that gene expression in their PBMCs displayed upregulation in granulopoiesis and IFN-related genes (39). This was followed by another study that revealed LDGs are able to produce and secrete IFN-α and the pro-inflammatory cytokines IL-1β and TNF-α. LDGs are able to induce vascular endothelial damage in SLE patients, thereby promoting pathogenesis [17]. We detected an extremely high percentage of LDGs in the PBMC fraction of the NEMO-deficient patient and showed that when compared to healthy neutrophils, LDGs expressed high levels of adhesion and neutrophil activation related genes, indicating that similar to LDGs characterized in SLE patients, these pathogenic cells contributed to tissue damage in the patient.

Neutrophils generate ROS as an antimicrobial defense mechanism to enable the killing of pathogens following phagocytosis [61]. ROS accumulation takes place at the priming stage in the life cycle of neutrophils and involves NADPH-oxidase activity [62]. Its build-up in NEMO-deficient untreated neutrophils compared to healthy untreated neutrophils, implies that the former spontaneously adopted a primed state, equipped to inflict tissue damage. Furthermore, our data showed an elevated type I IFN signature in the patient, as evidenced by increased levels of circulating IP-10 in the plasma, and increased ISG15/ISGylated proteins in PBMC lysates. LDGs were previously shown to release IFN-α in SLE patients [17]. Given the expansion in the LDG population and elevated type I interferon signature in our patient, it is conceivable that the chronic IFN signature in the NEMO-deficient patient stems also from LDGs.

Consistent with our findings on elevated type I IFN, a previous study on four patients with an exon 5 deletion in the *IKBKG* gene displayed an intermediate interferon response gene score comparable to CANDLE or SAVI patients. They identified binding sites for NF-κB1 at the IFN response genes *CXCL10*, *SOCS1*, *GBP1*, and hypothesized that the mutant NEMO protein binds and stabilizes TBK1 (TANK binding kinase 1), causing increased IRF3 phosphorylation and IFN secretion [52]. In our case, the patient acquired a stop codon rather than a deletion, which translates into an immune deficient phenotype. Nevertheless, the same mechanism could explain the elevated type I IFN signature in our patient.

The patient experienced CMV and tuberculosis infections in the course of his disease but responded to treatment and hence tested negative before undergoing transplantation. Nevertheless, since the patient suffered from immune deficiency, a chronically manifested clinically undetectable occult infection might also serve as a trigger for sustained type I IFN secretion. Given that NF-κB activation has also an important role in the regulation of inflammation, the compromised NF-κB signaling might have contributed to the persistency of the autoinflammation.

In conclusion, we identified for the first time that an expanded population of LDGs and activated neutrophils represent potential cellular sources underlying the clinical autoinflammatory pathophysiology in NEMO deficiency. In this respect, LDGs and/or activated neutrophils might also be key players contributing to NEMO colitis [14, 15]. We propose that the granulocytic dysregulation might be instigated by chronic type I IFN secretion stemming from either dysregulated NF-κB signaling and/or a clinically undetectable occult infection. Our findings reveal novel mechanisms leading to inflammatory manifestations in NEMO deficiency and offer alternative targets for diagnostic and therapeutic approaches.

Supplementary Information The online version contains supplementary material available at https://doi.org/10.1007/s10875-021-01176-3.

Acknowledgements This work was supported by the Scientific and Technological Research Council of Turkey (318S202) to S.B. We thank Ihsan Cihan Ayanoglu for his efforts and contributions in the NanoString gene expression panel analysis.

Author Contribution N.S.Y., B.K., S.B., and M.G. conceptualized and supervised the study. N.S.Y., B.K., B.G., I.C.Y, G.G.K., I.B., Y.A., D.C.K., R.J.H., and M.H. performed the experiments. S.B.E., A.P.S., A.K., E.N., N.K., O.D., A.D.Y., L.C., G.K., A.Y., B.S., E.K.A, and A.O. provided patient care, collected samples, and clinical data. N.S.Y., M.G., and S.B. wrote the paper. I.G., K.B. scientifically contributed to the manuscript. All authors reviewed and approved the final version of the manuscript.

Funding This work was supported by the Scientific and Technological Research Council of Turkey (318S202) to S.B.

Data Availability Available upon reasonable request to the corresponding authors.

Code Availability Not applicable.

Declarations

Ethics Approval The study was approved by Ethics Committee of Marmara University, School of Medicine. Written informed consents were obtained from the patient and parents.

Consent to Participate Informed consent for participation was obtained from all individuals.

Consent for Publication Informed consent for publication was obtained from all participants.

Conflict of Interest The authors declare no competing interests.

Additional Information Bar graphs, heatmaps, and volcano plots in this article were created with GraphPad Prism 8 software.

References

1. Karin M, Delhase M. The IκB kinase (IKK) and NF-κB: Key elements of proinflammatory signalling. Semin Immunol. 2000;12:85–98.
2. Liu T, Zhang L, Joo D, Sun SC. NF-κB signaling in inflammation. Signal Transduct Target Ther. 2017;2:e17023.
3. Schmitz ML, Krappmann D. Controlling NF-κB activation in T cells by costimulatory receptors. Cell Death Differ. 2006;13:834–42.
4. Luo JL, Kamata H, Karin M. IKK/NF-κB signaling: Balancing life and death - A new approach to cancer therapy. J Clin Invest. 2005;115:2625–32.
5. Bousfiha A, Jeddane L, Picard C, Al-Herz W, Ailal F, Chatila T, et al. Human Inborn Errors of Immunity: 2019 Update of the IUIS Phenotypical Classification. J Clin Immunol J Clin Immunol. 2020;40:66–81.
6. Döffinger R, Smahi A, Bessia C, Geissmann F, Feinberg J, Durandy A, et al. X-linked anhidrotic ectodermal dysplasia with immunodeficiency is caused by impaired NF-κB signaling. Nat Genet. 2001;27:277–85.
7. Smahl A, Courtols G, Vabres P, Yamaoka S, Heuertz S, Munnich A, et al. Genomic rearrangement in NEMO impairs NF-κB activation and is a cause of incontinentia pigmenti. Nature. 2000;405:466–72.
8. Zonana J, Elder ME, Schneider LC, Orlow SJ, Moss C, Golabi M, et al. A novel X-linked disorder of immune deficiency and hypohidrotic ectodermal dysplasia is allelic to incontinentia pigmenti and due to mutations in IKK-gamma (NEMO). Am J Hum Genet. 2000;67:1555–62.
9. Braue J, Murugesan V, Holland S, Patel N, Naik E, Leiding J, et al. NF-κB essential modulator deficiency leading to disseminated cutaneous atypical mycobacteria. Mediterr J Hematol Infect Dis. 2015;7:e2015010.
10. Huppmann AR, Leiding JW, Hsu AP, Raffeld M, Uzel G, Pittaluga S, et al. Pathologic findings in NEMO deficiency: A surgical and autopsy survey. Pediatr Dev Pathol. 2015;18:387–400.
11. Orange JS, Jain A, Ballas ZK, Schneider LC, Geha RS, Bonilla FA. The presentation and natural history of immunodeficiency caused by nuclear factor κB essential modulator mutation. J Allergy Clin Immunol. 2004;113:725–33.
12. Ramírez-Alejo N, Alcántara-Montiel JC, Yamazaki-Nakashimada M, Duran-McKinster C, Valenzuela-León P, Rivas-Larrauri F, et al. Novel hypomorphic mutation in IKBKG impairs NEMO-ubiquitylation causing ectodermal dysplasia, immunodeficiency, incontinentia pigmenti, and immune thrombocytopenic purpura. Clin Immunol. 2015;160:163–71.
13. Takada H, Nomura A, Ishimura M, Ichiyama M, Ohga S, Hara T. NEMO mutation as a cause of familial occurrence of Behçet's disease in female patients. Clin Genet. 2010;78:575–9.
14. Cheng LE, Kanwar B, Tcheurekdjian H, Grenert JP, Muskat M, Heyman MB, et al. Persistent systemic inflammation and atypical enterocolitis in patients with NEMO syndrome. Clin Immunol. 2009;132:124–31.
15. Nenci A, Becker C, Wullaert A, Gareus R, Van Loo G, Danese S, et al. Epithelial NEMO links innate immunity to chronic intestinal inflammation. Nature. 2007;446:557–61.
16. Fusco F, Pescatore A, Conte MI, Mirabelli P, Paciolla M, Esposito E, et al. EDA-ID and IP, Two Faces of the Same Coin: How the Same IKBKG / NEMO Mutation Affecting the NF-B Pathway Can Cause Immunodeficiency and/or Inflammation. Int Rev Immunol. 2015;34:445–59.
17. Denny MF, Yalavarthi S, Zhao W, Thacker SG, Anderson M, Sandy AR, et al. A Distinct Subset of Proinflammatory Neutrophils Isolated from Patients with Systemic Lupus Erythematosus Induces Vascular Damage and Synthesizes Type I IFNs. J Immunol. 2010;184:3284–97.
18. Mistry P, Nakabo S, O'Neil L, Goel RR, Jiang K, Carmona-Rivera C, et al. Transcriptomic, epigenetic, and functional analyses implicate neutrophil diversity in the pathogenesis of systemic lupus erythematosus. Proc Natl Acad Sci U S A. 2019;116:25222–8.
19. Rahman S, Sagar D, Hanna RN, Lightfoot YL, Mistry P, Smith CK, et al. Low-density granulocytes activate T cells and demonstrate a non-suppressive role in systemic lupus erythematosus. Ann Rheum Dis. 2019;78:957–66.
20. Rose T, Grützkau A, Hirseland H, Huscher D, Dähnrich C, Dzionek A, et al. IFNα and its response proteins, IP-10 and SIGLEC-1, are biomarkers of disease activity in systemic lupus erythematosus. Ann Rheum Dis. 2013;72:1639–45.
21. Lee-Kirsch MA. The Type i Interferonopathies. Annu Rev Med. 2017;68:297–315.
22. Kiykim A, Ogulur I, Dursun E, Charbonnier LM, Nain E, Cekic S, et al. Abatacept as a Long-Term Targeted Therapy for LRBA Deficiency. J Allergy Clin Immunol Pract. 2019;7:2790-2800.e15.
23. Ogulur I, Kiykim A, Baser D, Karakoc-Aydiner E, Ozen A, Baris S. Lymphocyte Subset Abnormalities in Pediatric-Onset Common Variable Immunodeficiency. Int Arch Allergy Immunol. 2020;181:228–37.

24. Yucel E, Karakus IS, Krolo A, Kiykim A, Heredia RJ, Tamay Z, et al. Novel Frameshift Autosomal Recessive Loss-of-Function Mutation in SMARCD2 Encoding a Chromatin Remodeling Factor Mediates Granulopoiesis. J Clin Immunol. 2021;41:59–65.
25. Kayaoglu B, Kasap N, Yilmaz NS, Charbonnier LM, Geckin B, Akcay A, et al. Stepwise Reversal of Immune Dysregulation Due to STAT1 Gain-of-Function Mutation Following Ruxolitinib Bridge Therapy and Transplantation. J Clin Immunol. 2021;769–779.
26. Klemann C, Pannicke U, Morris-Rosendahl DJ, Vlantis K, Rizzi M, Uhlig H, et al. Transplantation from a symptomatic carrier sister restores host defenses but does not prevent colitis in NEMO deficiency. Clin Immunol. 2016;164:52–6.
27. Gustafson MP, Lin Y, Maas ML, Van Keulen VP, Johnston PB, Peikert T, et al. A method for identification and analysis of non-overlapping myeloid immunophenotypes in humans. PLoS One. 2015;10:e0121546.
28. Wither JE, Prokopec SD, Noamani B, Chang NH, Bonilla D, Touma Z, et al. Identification of a neutrophil-related gene expression signature that is enriched in adult systemic lupus erythematosus patients with active nephritis: Clinical/pathologic associations and etiologic mechanisms. PLoS One. 2018;13:e0196117.
29. Hacbarth E, Kajdacsy-Balla A. Low density neutrophils in patients with systemic lupus erythematosus, rheumatoid arthritis, and acute rheumatic fever. Arthritis Rheum. 1986;29:1334–42.
30. Bennett L, Palucka AK, Arce E, Cantrell V, Borvak J, Banchereau J, et al. Interferon and granulopoiesis signatures in systemic lupus erythematosus blood. J Exp Med. 2003;197:711–23.
31. Kegerreis BJ, Catalina MD, Geraci NS, Bachali P, Lipsky PE, Grammer AC. Genomic Identification of Low-Density Granulocytes and Analysis of Their Role in the Pathogenesis of Systemic Lupus Erythematosus. J Immunol. 2019;202:3309–17.
32. Kruzel ML, Zimecki M, Actor JK. Lactoferrin in a context of inflammation-induced pathology. Front Immunol. 2017;8:1438.
33. Holzinger D, Foell D, Kessel C. The role of S100 proteins in the pathogenesis and monitoring of autoinflammatory diseases. Mol Cell Pediatr. 2018;5:7.
34. Pandey R, Zhou M, Islam S, Chen B, Barker NK, Langlais P, et al. Carcinoembryonic antigen cell adhesion molecule 6 (CEACAM6) in Pancreatic Ductal Adenocarcinoma (PDA): An integrative analysis of a novel therapeutic target. Sci Rep. 2019;9:18347.
35. Skubitz KM, Skubitz APN. Interdependency of CEACAM-1, -3, -6, and -8 induced human neutrophil adhesion to endothelial cells. J Transl Med. 2008;6:78.
36. Tardif MR, Chapeton-Montes JA, Posvandzic A, Pagé N, Gilbert C, Tessier PA. Secretion of S100A8, S100A9, and S100A12 by Neutrophils Involves Reactive Oxygen Species and Potassium Efflux. J Immunol Res. 2015;2015:296149.
37 Babior BM, Kipnes RS, Curnutte JT. Biological defense mechanisms The production by leukocytes of superoxide a potential bactericidal agent. J Clin Invest. 1973;52:741–4.
38. Hidalgo A, Chilvers ER, Summers C, Koenderman L. The Neutrophil Life Cycle. Trends Immunol. 2019;40:584–97.
39. Korkmaz B, Horwitz MS, Jenne DE, Gauthier F. Neutrophil elastase, proteinase 3, and cathepsin G as therapeutic targets in human diseases. Pharmacol Rev. 2010;62:726–59.
40. Gul E, Sayar EH, Gungor B, Eroglu FK, Surucu N, Keles S, et al. Type I IFN–related NETosis in ataxia telangiectasia and Artemis deficiency. J Allergy Clin Immunol. 2018;142:246–57.
41. Loeb KR, Haas AL. The interferon-inducible 15-kDa ubiquitin homolog conjugates to intracellular proteins. J Biol Chem. 1992;267:7806–13.
42. Lenschow DJ, Lai C, Frias-Staheli N, Giannakopoulos NV, Lutz A, Wolff T, et al. IFN-stimulated gene 15 functions as a critical antiviral molecule against influenza, herpes, and Sindbis viruses. Proc Natl Acad Sci U S A. 2007;104:1371–6.
43. Perng YC, Lenschow DJ. ISG15 in antiviral immunity and beyond. Nat Rev Microbiol. 2018;16:423–39.
44. Liu M, Guo S, Hibbert JM, Jain V, Singh N, Wilson NO, et al. CXCL10/IP-10 in infectious diseases pathogenesis and potential therapeutic implications. Cytokine Growth Factor Rev. 2011;22:121–30.
45. Hanson EP, Monaco-Shawver L, Solt LA, Madge LA, Banerjee PP, May MJ, et al. Hypomorphic NEMO mutation database and reconstitution system identifies phenotypic and immunologic diversity. J Allergy Clin Immunol. 2008;122:1169.
46. Barczewski AH, Ragusa MJ, Mierke DF, Pellegrini M. The IKK-binding domain of NEMO is an irregular coiled coil with a dynamic binding interface. Sci Rep. 2019;9:2950.
47. Maubach G, Schmädicke AC, Naumann M. NEMO Links Nuclear Factor-κB to Human Diseases. Trends Mol Med. 2017;23:1138–55.
48. Li XH, Fang X, Gaynor RB. Role of IKKγ/NEMO in Assembly of the IκB Kinase Complex. J Biol Chem. 2001;276:4494–500.
49. Rushe M, Silvian L, Bixler S, Chen LL, Cheung A, Bowes S, et al. Structure of a NEMO/IKK-Associating Domain Reveals Architecture of the Interaction Site. Structure. 2008;16:798–808.
50. Rothwarf DM, Zandi E, Natoli G, Karin M. IKK-γ is an essential regulatory subunit of the IκB kinase complex. Nature. 1998;395:297–300.
51. Wu C-J, Conze DB, Li T, Srinivasula SM, Ashwell JD. Sensing of Lys 63-linked polyubiquitination by NEMO is a key event in NF-κB activation. Nat Cell Biol. 2006;8:398–406.
52. de Jesus AA, Hou Y, Brooks S, Malle L, Biancotto A, Huang Y, et al. Distinct interferon signatures and cytokine patterns define additional systemic autoinflammatory diseases. J Clin Invest. 2020;130:1669–82.
53. Nelson RT, Boyd J, Gladue RP, Paradis T, Thomas R, Cunningham AC, et al. Genomic Organization of the CC Chemokine MIP-3α/CCL20/LARC/EXODUS/SCYA20, Showing Gene Structure, Splice Variants, and Chromosome Localization. Genomics. 2001;73:28–37.
54. Hieshima K, Imai T, Opdenakker G, Van Damme J, Kusuda J, Tei H, et al. Molecular Cloning of a Novel Human CC Chemokine Liver and Activation-regulated Chemokine (LARC) Expressed in Liver: Chemotactic Activity for Lymphocytes and Gene Localization on chromosome 2. J Biol Chem. 1997;272:5846–53.
55. Croft M. Costimulation of T cells by OX40, 4–1BB, and CD27. Cytokine Growth Factor Rev. 2003;14:265–73.
56. Devin A, Cook A, Lin Y, Rodriguez Y, Kelliher M. Liu Z gang The Distinct Roles of TRAF2 and RIP in IKK Activation by TNF-R1: TRAF2 Recruits IKK to TNF-R1 while RIP Mediates IKK Activation. Immunity. 2000;12:419–29.
57. Masson PL, Heremans JF, Schonne E. Lactoferrin, an Iron-Binding Protein in Neutrophilic Leukocytes. J Exp Med. 1969;130:643–58.
58. Flo TH, Smith KD, Sato S, Rodriguez DJ, Holmes MA, Strong RK, et al. Lipocalin 2 mediates an innate immune response to bacterial infection by sequestrating iron. Nature. 2004;432:917–21.
59. Starkey PM, Barrett AJ. Human cathepsin G. Catalytic and immunological properties Biochem J. 1976;155:273.
60. Brignone C, Munoz O, Batoz M, Rouquette-Jazdanian A, Cousin J-L. Proteases produced by activated neutrophils release soluble CD23 fragments endowed with proinflammatory effects. FASEB J. 2001;15:2027–9.
61. Rosales C. Neutrophil: A cell with many roles in inflammation or several cell types? Front Physiol. 2018;9:113.
62. Condliffe AM, Kitchen E, Chilvers ER. Neutrophil priming: Pathophysiological consequences and underlying mechanisms. Clin Sci. 1998;94:461–71.

Authors and Affiliations

Naz Surucu Yilmaz[1] · Sevgi Bilgic Eltan[2,3,4] · Basak Kayaoglu[1] · Busranur Geckin[1] · Raul Jimenez Heredia[5,6,7,8] · Asena Pinar Sefer[2,3,4] · Ayca Kiykim[9] · Ercan Nain[2,3,4] · Nurhan Kasap[2,3,4] · Omer Dogru[10] · Ayse Deniz Yucelten[11] · Leyla Cinel[12] · Gulsun Karasu[13] · Akif Yesilipek[13] · Betul Sozeri[14] · Goksu Gokberk Kaya[15] · Ismail Cem Yilmaz[1] · Ilayda Baydemir[1] · Yagmur Aydin[1] · Deniz Cansen Kahraman[16] · Matthias Haimel[5,7] · Kaan Boztug[5,6,7,8,17] · Elif Karakoc-Aydiner[2,3,4] · Ihsan Gursel[15] · Ahmet Ozen[2,3,4] · Safa Baris[2,3,4] · Mayda Gursel[1]

[1] Department of Biological Sciences, Middle East Technical University, B-58, Üniversiteler Mah. Dumlupınar Bulvarı No:1, Ankara, Turkey

[2] Division of Pediatric Allergy and Immunology, Marmara University, Fevzi Çakmak Mah. No: 41, Istanbul, Turkey

[3] Istanbul Jeffrey Modell Diagnostic and Research Center for Primary Immunodeficiencies, Istanbul, Turkey

[4] The Isil Berat Barlan Center for Translational Medicine, Istanbul, Turkey

[5] Ludwig Boltzmann Institute for Rare and Undiagnosed Diseases, Vienna, Austria

[6] St. Anna Children's Cancer Research Institute (CCRI), Vienna, Austria

[7] CeMM Research Center for Molecular Medicine of the Austrian Academy of Sciences, Vienna, Austria

[8] Department of Pediatrics and Adolescent Medicine, Medical University of Vienna, Vienna, Austria

[9] Faculty of Medicine, Pediatric Allergy and Immunology, Istanbul University-Cerrahpasa, Istanbul, Turkey

[10] Division of Pediatric Hematology-Oncology, Marmara University, Istanbul, Turkey

[11] Division of Dermatology, Marmara University, Istanbul, Turkey

[12] Division of Pathology, Marmara University, Istanbul, Turkey

[13] Goztepe Medicalpark Hospital, Pediatric Stem Cell Transplantation Unit, İstanbul, Turkey

[14] Division of Pediatric Rheumatology, University of Health Sciences, Umraniye Research and Training Hospital, Istanbul, Turkey

[15] Therapeutic ODN Research Lab, Department of Molecular Biology and Genetics, Bilkent University, Bilkent 06800, Ankara, Turkey

[16] KanSiL, Department of Health Informatics, Graduate School of Informatics, Middle East Technical University, Ankara, Turkey

[17] St. Anna Children's Hospital, Department of Pediatrics and Adolescent Medicine, Medical University of Vienna, Vienna, Austria